4-17-2024

Comparison of Wet Downburst Wind Event and Non-Severe Thunderstorm Characterisics using MRMS Radar Products

Eliana Raisa Carter
University of Alabama in Huntsville

Comparison of Wet Downburst Wind Event and Non-Severe Thunderstorm Characteristics using MRMS Radar Products

by

Eliana Raisa Carter

An Honors Capstone
submitted in partial fulfillment of the requirements
for the Honors Diploma
to
The Honors College
of
The University of Alabama in Huntsville
04/17/24
Honors Capstone Project Director: Dr. Lawrence Carey

_Eliana Carter________04/17/24______________________________

Student Date

Digitally signed by Lawrence D. Carey
Date: 2024.04.18 13:43:30 -05'00'

Project Director (signature) Date

Digitally signed by Lawrence D. Carey
Date: 2024.04.18 13:43:58 -05'00'

Department Chair (signature) Date

Digitally signed by Sean M Lane
Date: 2024.04.25 17:39:56 -05'00'

Honors College Dean (signature) Date

Honors College

Frank Franz Hall

+1 (256) 824-6450 (voice)

+1 (256) 824-7339 (fax)

honors@uah.edu

Honors Thesis Copyright Permission

This form must be signed by the student and submitted with the final manuscript.

In presenting this thesis in partial fulfillment of the requirements for Honors Diploma or Certificate from The University of Alabama in Huntsville, I agree that the Library of this University shall make it freely available for inspection. I further agree that permission for extensive copying for scholarly purposes may be granted by my advisor or, in his/her absence, by the Chair of the Department, Director of the Program, or the Dean of the Honors College. It is also understood that due recognition shall be given to me and to The University of Alabama in Huntsville in any scholarly use which may be made of any material in this thesis.

_Eliana_Carter____________________

Student Name (printed)

_Eliana Carter________________________

Student Signature

__04/17/24________________________

Date

Table of Contents

Abstract

Downbursts, both dry and wet, are a subset of severe straight line wind events that cause quite a bit of damage. Reported impacts include hundreds of downed trees, carport damage, and even shattered vehicle windows. These short-lived storms are difficult to detect with the current limitations of singular radars and sparse Automated Surface Observation Systems (ASOS). Multi Radar Multi Sensor (MRMS) Radar is a system that combines observations from multiple sources (surface, air, satellite), meteorological model input, lightning detection, and data from multiple radars to provide a more complete picture of weather phenomena. The research process began with collecting a sample set of 27 wet downburst cases via the Storm Prediction Center (SPC) severe report archive and analysis of the radar data in GR2 Analyst. Once these cases were documented, corresponding MRMS archive files were downloaded and five MRMS Radar products were chosen for analysis: 30 dBZ Echo Top, Reflectivity at -10°C, Vertically Integrated Ice (VII), Vertically Integrated Liquid (VIL), and Vertically Integrated Liquid Density (VILD, or VIL scaled to a storm's height). Python code was then used to generate plots, figures, and a data frame for interpretation. These initial figures suggest that VILD and Reflectivity at -10°C may be useful for wet downburst detection, however, research involving null cases was needed for comparison. The focus of this capstone project was to identify and analyze non-severe storm cases for comparison. This process was very similar, however, county populations, a lack of SPC reports, and a lack of National Weather Service (NWS) warnings helped ensure non-severity of the sample. Once both datasets were collected, final comparison appeared to show favorable distinctions for the following MRMS Radar products: EchoTop at 30 dBZ, VII, and Reflectivity at -10°C. There is noticeable separation between the severe and non-severe datasets for these products, which may prove useful in future wet downburst detection upon further investigation.

Introduction

In August of 2012, the student researcher went on a camping trip that would change her life forever. During the first afternoon of this trip with her family, a dangerous storm cropped up, leaving the researcher and present family members to seek shelter on a cabin porch. Not understanding what had happened, the researcher was traumatized for an entire year. However, over this same year, she began to learn about what she was so afraid of. This fear blossomed into a fascination of weather and a realization that this dangerous storm had been a wet downburst (Figure 1)! Wet downbursts can be very dangerous; they come and go quickly, usually have little warning, and they cause widespread damage. Some damage reports have even included remarks such as hundreds of trees being downed, carports sustaining damage, and even shattered car windows. This led to a search to better understand how downbursts form, and why they are so difficult to forecast.

Downbursts tend to have a few main catalysts. The first of these initiation processes is called precipitation loading. This occurs when the amount of precipitation (water, and especially ice particles) becomes too heavy for the storm's updraft to support them anymore. This results in precipitation and strong winds to come crashing to the ground, with the strong winds spreading out in all directions. The next initiation process is known as evaporative cooling (Figure 2). Evaporative cooling occurs when precipitation encounters air with low relative humidity. This drier air causes some of the water droplets to evaporate, cooling the air and causing it to sink. This can quickly enhance a downdraft, leading to a full scale downburst (US Department of Commerce). A third driving mechanism is known as melting. Similar to evaporative cooling, the melting of hail and/or ice particles within a cloud causes the surrounding air to cool. Since cooler air is more dense, it creates a sinking motion that enhances the downdraft, which can create a downburst scenario. Understanding the initiation process of a downburst leads to the question of what makes them so difficult to forecast, aside from their short lifespan.

The issue of downburst detection boils down to two major limitations: the sparse distribution of ASOS stations (in comparison to reports and storm locations), and the limitations of a singular radar. The prior issue is discussed in Smith et al. 2013, which explores severe thunderstorm wind gust climatology (various modes of storms) as well as how these wind events are reported. Most notably, the results describe a major discrepancy between the frequency and location of reports from the *Storm Data* severe wind database and the frequency and location of reports from ASOS/AWOS stations during the years 2003-2009 (Figure 3). As useful as these station sensors are at detecting meteorological data, they are usually placed at airports or on top of open, level ground. This is to help avoid interference with data collection (uneven ground, topography interference, trees blocking valuable data, etc.). This leads to a more sparse distribution and to people reporting more severe wind events than ASOS stations in densely populated areas such as the eastern United States (Figure 3). The latter issue is the limitations of a singular radar. After an emitted pulse makes its journey away from the radar, the earth's surface curves away from the beam. The beam is also traveling at a fixed elevation angle to capture different layers of data. This is a limitation because if a storm is too close to or too far from the radar (outside a range of 30-120 km), critical data can be lost. The top of a storm's reflectivity values can be cut off or even overshot completely. Another limitation of a singular radar is the dreaded "cone of silence". With the exception of some research radars that point straight upwards, radars cannot collect data from storms that pass directly overhead. This is another critical loss of data, especially if a storm is evolving while passing over the radar.

These limitations beg the question of what can be done to minimize loss of data. One such product that can do this is the Multi Radar Multi Sensor (MRMS) product. This product was developed by the NOAA National Severe Storms Laboratory (NSSL). It uses "fully automated algorithms"[1] to combine multi-radar data, surface observations, upper air observations, lightning detection systems, satellite data, forecast models, and 2D multi-sensor data in order to generate mosaics of radar data for storage and future analysis (Multi-Radar/Multi-Sensor System (MRMS); Zhang et al. 2016; Smith et al. 2016). The nature of this product allows it to have a more comprehensive overview of weather phenomena versus a singular radar or even network of ASOS stations. The goal of this research is to use selected MRMS Radar products to differentiate between wet downburst and non-severe storm samples. This information will be used to help identify best MRMS Radar products for further investigation into forecast potential.

Methods

The research process for collecting the necessary data samples was broken up into two segments - the first focusing on wet downburst cases, and the second focusing on identifying null cases to conduct a comparison of the two samples. All cases were limited to the warm seasons (approximately March through September) of 2020 to 2022. This is due to the fact that the MRMS data archive only extends back to the fall of 2019. The research process also began in 2022, and warmer season storms are more likely to have cellular convection as their driving mechanism. To begin the first segment of the research process, a criteria was chosen to identify wet downburst cases. The storms were verified to have been downbursts, by ensuring the Storm Prediction Center (SPC) severe report database included the term microburst or downburst for each case. There was a case or two that resulted from an in-person report (researcher's hometown hit by microburst) that was verified in GR2 Analyst and/or through online news reports. Each case was required to be cellular in nature (at least semi-isolated), and not a Quasi-Linear Convective System, supercell, mid-latitude cyclone, dry downburst, or tornado-producing storm. This was to ensure the storm cell itself was responsible for the event and to make sure proper driving mechanisms were in place. The other storm types have a completely different nature than the desired downburst cases. Due to common report errors, storms were allowed to be within a 20 minute window from the report time - given the storm passed near the report coordinates. The storms were typically no more than 10 minutes away from the report, if not at the same time. Provided wind speeds in a case report were considered ideal, but not required as there were not many. Damage reports were also helpful in determining the impact of wet downburst wind events.

Once cases were identified in the SPC severe report archive, level II Nexrad data was downloaded for each case from the AWS S3 Explorer database (AWS S3 Explorer). The data was loaded into GR2 Analyst to document each storm's characteristics. To ensure accuracy in the GR2 radar data analysis, storms were required to be 30-120 km from the radar. Anything outside of this range was typically excluded; a handful of exceptions were made for storms that exceeded 120 km, but still retained decent structure and resolution. Nearest radar location to the given storm proved to be a challenge at times. As the cases were analyzed (a total of 27 cases were collected), their characteristics were documented, and screen captures of the radar data were stored by case. Documented information included: case number, state, county, date, report time (UTC), report coordinates, the timing of storm intersection at a report location (UTC), distance of a storm from the radar (nautical miles, km), radar name, peak VIL analysis time (UTC, VIL peaks then drastically drops during a downburst event), MRMS bounds (these were set at peak VIL analysis time), wind speed when provided, severity based on severe storm criteria if wind speeds were provided (Thunderstorm Basics), and specific damage reports or notes for each case (Table 1).

At the same time as collecting case information, the student researcher was taught basic python coding. Through the tutoring and tools provided by her peers, the student researcher was able to develop python code to process the MRMS data for each case. This code had five primary objectives: to store case information in a dictionary (name, timestamp, bounds), to store MRMS product information in a dictionary (bounds, units, title, histogram plot color), to plot MRMS product values for each case, to store maximum product values by case and product in a data frame, and to plot histograms for each MRMS radar product (for all cases in the dictionary).

Once the coding and case selection processes were complete, the student researcher began downloading MRMS files that corresponded to the date and UTC hour of each case. Once these files were downloaded, they were extracted into their respective folders, and the same five MRMS product files were isolated for use. The code was then run to generate the plots, data frame, and histogram charts for all of the cases and all five MRMS products. The data frame information was also output to an excel spreadsheet to manually create a statistics chart of the mean, minimum, and maximum values for each MRMS product and all of the cases. One important note is that although 27 cases were collected, 26 were used for analysis. This is due to the case in Beltrami, MN, affectionately nicknamed “Beltrami”. Beltrami had statistics that were off the charts in comparison to all of the other cases. After further analysis, the storm appeared to be supercellular in nature with an embedded downburst - a very different driving mechanism and intensity than the typical wet downburst event. This case greatly skewed the data, making it difficult to interpret, and Beltrami a significant outlier (even from stronger downburst events). This case was removed from the analysis and plotting process.

The second segment of the research process was very similar to the first. However, there were differences due to the unique nature of non-severe thunderstorms. The biggest problem with this part of the research process is that nobody reports non-severe thunderstorms. This leaves the case collection process up to the researcher - a situation that can easily lead to bias. To limit, and hopefully avoid, this risk of bias, any collected cases were required to meet the following criteria. Any given case must: be passing over a well-populated county (researcher attempted to stick to about 40k residents at minimum - more is better), to be at least 45 km away from any SPC severe report, and to have no National Weather Service (NWS) warnings. Cases were also selected at their peak levels of reflectivity over the well-populated county. This was to ensure that some level of convection was present in the cases. The data sample was again limited to the warm seasons of 2020 to 2022, and most cases were during the afternoon hours due to the weaker driving mechanism (weaker convection) in non-severe thunderstorms. Cases were also required to be within the same distance limits (30-120 km) from the selected radar, and to be cellular in nature with absolutely no severe qualities (no downbursts, QLCS patterns, tornadoes, severe reports, or supercells).

The case selection process began with identifying convective days through both the Iowa State IEM Nexrad Mosaic and the SPC severe report archives. Once a region was located, and was relatively clear of severe reports, level II Nexrad radar data was loaded into GR2 analyst during the time period on the IEM Nexrad Mosaic loop. If a storm case met the prior criteria and passed over a populated county during moderate to peak intensity, it was chosen as a case and its characteristics were recorded. 20 cases were collected for the null data sample, with the following information documented: case number, state, county, date, county population, time of storm over location (UTC), location coordinates, radar, distance from radar (nautical miles, km), MRMS bounds (not recorded based on VIL, as the null cases did not have much to begin with), and notes on the storm (Table 2).

Once all of the non-severe cases were collected, a copy of the previously written code was made in order to customize it to the non-severe data sample. A new case dictionary was created with all of the same parameters as in the first code. As this code was being tailored to the new cases, corresponding MRMS data files were also downloaded for each case. These files were extracted, with the same five MRMS product files being isolated for the code to use. With the MRMS product files and code being ready, the code was run to produce plots, histograms, and a data frame for the new data sample. Lastly, the data frame was once again output to an excel spreadsheet to create the same statistical charts for the null cases as well as combined histograms and statistical charts - these included both the downburst and null data samples for final comparison.

The five MRMS radar products chosen for analysis were: Vertically Integrated Ice (VII), Vertically Integrated Liquid (VIL), Vertically Integrated Liquid Density (VILD), Reflectivity at -10°C (Reflectivity_-10) , and EchoTop at 30dBZ (EchoTop_30). These products were each chosen for their unique potential ties to downburst formation. The first product, VII, is a radar derived product that estimates the amount of ice particles in a cloud. This integration covers the -10 to -40°C layer, or the graupel and ice growth region. VII has been previously linked to hail and lightning formation (MRMS Products Guide). Since ice melting and cooler air both initiate downbursts, VII may also relate to downburst formation. The next product, VIL, is similar to VII except that this time a sum is used to calculate the amount of liquid water within a cloud, not ice, using a reflectivity-derived relationship (MRMS Products Guide). VIL rapidly decreases after a downburst occurs, meaning a peak and drop should happen in quick succession. Knowing the amount of peak liquid content in a downburst versus a non-severe thunderstorm may prove quite useful. VILD is the same as VIL, except it is scaled to the height of the storm (MRMS Products Guide). This gives a more accurate depiction of water concentration in a cloud, since storms have varying heights and can even be quite shallow. Next, EchoTop at 30 dBZ shows the top height of the storm's precipitation layer where 30 dBZ reflectivity is detected (MRMS Products Guide). This is extremely useful because storm heights help detect a storm's updraft intensity, overshooting tops, and if a storm is strengthening or weakening. Similar to VIL, EchoTop at 30 dBZ should also sharply decrease after a downburst occurs. Last but certainly not least is Reflectivity at -10°C. Reflectivity at the -10°C level is reflectivity at the beginning of the graupel and ice growth region. This data is useful in detecting ice growth and hail cores, which are both capable of producing downbursts via cooling, melting, drag, and precipitation loading (MRMS Products Guide). Each of these five products were used to analyze both data samples and can be seen in the tables and charts below.

Results

One of the first results that came out of this study were the individual histograms for each MRMS product and each data set. The first set of individual histograms were generated for the downburst sample. The EchoTop 30 histogram for the downburst sample had a pretty broad distribution with a peak value of 19 km (Figure 4). There were multiple peaks in this histogram, implying that there may not be a clear distinction between downburst and null cases. The next downburst histogram was VII. VII was heavily skewed towards lower values with a peak value of 91.9 kg/m^2. This chart certainly shows a pattern where most of the cases leaned towards lower values, which could show a distinction only if null cases have lower values on average (since weaker convection is not likely to have larger values) (Figure 4). The third downburst histogram was for VIL. Like EchoTop 30, VIL also had a fairly broad distribution but with bimodal peaks this time. VIL had a peak value of 60.6 kg/m^2, and a pattern cannot be clearly distinguished without null cases for comparison (Figure 4). The fourth downburst histogram chart was for VILD. VILD seems to be negatively skewed towards larger values with a peak value of 2.3 g/m^3. This may prove useful, as it is likely weaker convection will lead to lower concentrations of VIL. However, this may not be the case since VILD is only a scaled version of VIL, which has a fairly broad distribution (Figure 4). The last downburst histogram chart was for Reflectivity at -10°C. Reflectivity at -10°C seemed to also be slightly skewed towards larger values with two separate peaks and a peak value of 65 dBZ. Although it seems to have a slightly broader distribution than VII or VILD, it is important to note that the histogram begins at about 45 dBZ. Every single downburst case has values around or greater than 50 dBZ, which can be a significant indicator when compared to null cases.

The second set of individual histograms were generated for the non-severe or null case sample. Interestingly, the EchoTop 30 histogram for the null sample also had a pretty broad distribution with a peak value of 19 km (Figure 5). There was one main peak in this histogram, and there may not be a clear distinction between downburst and null cases. The next null histogram was for VII. VII was even more heavily skewed towards lower values than the downburst cases with a peak value of 35.5 kg/m^2. Although this chart shows a similar distribution to the downburst VII chart, the chart values are much lower, meaning there will be a separation between the data sets (Figure 5). The third null histogram was for VIL. Like EchoTop

30, VIL also had a fairly broad distribution but with two peaks towards the lower spectrum of values. VIL had a peak value of 53.6 kg/m^2, and a pattern cannot be clearly distinguished without comparison of both data sets (Figure 5). The fourth null histogram chart was for VILD. VILD seems to be split with a bimodal distribution that has peaks in both lower and higher values. This data sample has a peak value of 3.1 g/m^3 - even higher than the downburst peak! This may not prove useful as hoped, but VILD is still a scaled version of VIL so combined analysis is needed (Figure 5). The last null histogram chart was for Reflectivity at -10°C. Reflectivity at -10°C seemed to have a fairly similar distribution to the downburst cases, but the values seem to be shifted slightly lower. This sample set had a peak value of 59 dBZ (Figure 5).

The next portion of the results is the statistical analysis charts for each sample set. The charts show the data sample's mean, min, and max for each of the five selected MRMS products. The mean, minimum, and maximum values for each product and sample set can be found below in Figure 6 and Figure 7 for a typical downburst storm and non-severe storm, respectively. These results will be further explored and compared in the final combination statistical analysis chart.

The final and most important results from this entire study are the combined histogram and statistical analysis charts. Each of these charts work the same way as the individual histograms, except they combine both data samples for comparison. The first histogram is for the combined EchoTop 30. This chart seems to contain a bit of overlap, however, each sample set has a singular peak, and are somewhat separated. The null cases seem to have a bell curve distribution and peak in the lower to moderate values, while the downburst cases seem to have a peak (maybe a second at the end) in the moderate to larger values (Figure 8). Since EchoTop is an indicator of updraft and storm intensity, this seems to imply that despite some overlap, downbursts will tend to have higher dBZ echo tops and higher overall intensity than non-severe thunderstorms. The next histogram is for combined analysis of VII. In this chart, there is also a moderate degree of separation despite both sample sets being positively skewed towards smaller values. The null sample set has a very strong peak at values of 0-10 kg/m^2, which is before the downburst sample set begins, and implies that most of the null cases had significantly lower values than the downburst sample set (Figure 8). The next two combined histogram charts represent VIL and VILD. Both of these charts still have a relatively broad distribution of both sample sets. It is rather difficult to distinguish any relationship between the two sample sets, meaning VIL and VILD are likely not the best indicators of a downburst event occurring (Figure 8). The last combined histogram chart represents Reflectivity at -10°C. Reflectivity at -10°C appears to have almost the opposite distribution of VII. There appears to be a significant degree of separation between the two sample sets despite some overlap, with both sample sets being negatively skewed towards larger values. Most null cases are contained within the low to moderate reflectivity values, however, downburst cases only begin to show up around 50 dBZ (Figure 8). This seems to show a solid distinction between the downburst cases and the non-severe cases.

The combined statistical chart represents the mean and median of both sample sets and for each selected MRMS radar product (Figure 9). Although the mean represents the average value of a data set, the median was also included in case the mean was biased by any potential outliers, especially due to the smaller sample size. A statistical T-test was considered, but due to lack of experience and time, it was not conducted. In both charts, downburst cases possessed larger mean and median values across the board (Figure 9). The radar products that appeared to have the largest distinction in both charts were VII, VIL, and VILD (a scaled value). Due to distributions, VIL and VILD are still difficult to make any distinctions with due to their broad distributions.

As with any research study, there were potential sources of error in this study. The first of which being uncertainty in some of the downburst cases. One example is a case in Jones, NC that was a merger storm at the time of the report. This can cause uncertainty of which cell caused the report, whether they were fully merged yet, and if the driving mechanisms of the downburst were the same. Another case was in Tooele, UT. There was one strong and clear cell that passed through the area, and across the same road at the report time, but 10 km away. The reporter would have driven through this storm, and it was clearly the source of the report, however, this does lend a level of uncertainty. Other potential sources of error are the limited sample size of this study (more data would be necessary to draw any decisive conclusions), potential unintended bias in case selection, and other human or technological sources of error. The student-researcher developed criteria and took time to minimize any sources of error, however it is still possible.

Conclusions

Wet downburst wind events come and go quickly and can cause a lot of damage - even as much if not more than some tornadoes. Despite the difficulty of forecasting these storms, more research into this subject can lead to new ways of identifying downbursts, to learning cool information about the storms, and to more lead time, increasing public awareness and safety. Although ASOS stations and singular radars have limitations, MRMS radar products may be able to help bridge the gap and provide useful insights into future downburst detection. Out of the five MRMS radar products selected for this study, EchoTop at 30 dBZ, VII, and Reflectivity at -10°C appear to be the most promising for future investigation. This is due to their distributions and having some of the most clear distinctions between the null and downburst sample sets. Further investigation and research may involve larger sample sets, new parameters, different MRMS products, and maybe eventually the development of an algorithm to use relevant MRMS products for downburst detection.

References

AWS S3 Explorer. https://noaa-nexrad-level2.s3.amazonaws.com/index.html (Accessed April 17, 2024).

Multi-Radar/Multi-Sensor System (MRMS). *NOAA National Severe Storms Laboratory*,. https://www.nssl.noaa.gov/projects/mrms/ (Accessed April 28, 2023).

MRMS Products Guide - Warning Decision Training Division (WDTD) - Virtual Lab. https://vlab.noaa.gov/web/wdtd/mrms-products-guide (Accessed April 28, 2023).

Smith, B. T., T. E. Castellanos, A. C. Winters, C. M. Mead, A. R. Dean, and R. L. Thompson, 2013: Measured Severe Convective Wind Climatology and Associated Convective Modes of Thunderstorms in the Contiguous United States, 2003–09. *Weather and Forecasting*, **28**, 229–236, https://doi.org/10.1175/WAF-D-12-00096.1.

Smith, T. M., and Coauthors, 2016: Multi-Radar Multi-Sensor (MRMS) Severe Weather and Aviation Products: Initial Operating Capabilities. *Bulletin of the American Meteorological Society*, **97**, 1617–1630, https://doi.org/10.1175/BAMS-D-14-00173.1.

Thunderstorm Basics. *NOAA National Severe Storms Laboratory*,. https://www.nssl.noaa.gov/education/svrwx101/thunderstorms/ (Accessed April 28, 2023).

US Department of Commerce, N., How Do Downbursts Form? https://www.weather.gov/lmk/downburst (Accessed April 28, 2023).

US Department of Commerce, N., Straight-Line Winds vs. Tornado: What's the Difference? https://www.weather.gov/iwx/2013_straight-line_winds_vs_tornado (Accessed April 17, 2024).

Zhang, J., and Coauthors, 2016: Multi-Radar Multi-Sensor (MRMS) Quantitative Precipitation Estimation: Initial Operating Capabilities. *Bulletin of the American Meteorological Society*, **97**, 621–638, https://doi.org/10.1175/BAMS-D-14-00174.1.

Tables

Tables of case documentation are too large to include in this write up. Links will be provided to the Google Sheets of each. The spreadsheets should be link-accessed - please contact the student-researcher if this is not the case.

https://docs.google.com/spreadsheets/d/1jq9PEIzW2LSsgt6VwIbu-GLKBkyQKyRtI36Y9K7etoE/edit?usp=sharing
Table 1: Case documentation for wet downburst cases.

https://docs.google.com/spreadsheets/d/1sEufrXBtZLKAcP7CaBciwjZWMmYumfbmR3J3AZGYnLc/edit?usp=sharing
Table 2: Case documentation for null cases (non-severe thunderstorms).

	case_name	time_stamp	VIL	VII	VIL_Density	Reflectivity_-10C	EchoTop_30	month	hour
0	Davidson_TN	7/26/21 20:18	24.1	11.2	1.6	54	15	7	20
1	Williamson_TX	7/28/21 21:26	36	19.2	2.6	57	14.5	7	21
2	Washington_PA	8/8/21 20:58	32.1	22.4	2.2	61	14	8	20
3	Northampton_PA	7/17/21 19:00	37.6	25.9	2.5	57.5	14	7	19
4	Ulster_NY	5/15/20 23:20	17.9	6.5	2	48	9	5	23
5	Broward_FL	5/16/20 22:34	25.4	13.8	2.8	56.5	14	5	22
6	Washington_CO	6/9/20 5:56	32.5	28	2.5	58.5	14	6	5
7	Lancaster_NE	6/18/20 18:24	43.4	41.2	2.8	62	16	6	18
8	Tooele_	7/24/20	19.2	9.7	1.8	55	12	7	0

	UT	0:08							
9	Parker_TX	8/29/20 23:52	61.9	91.9	3.9	65	17	8	23
10	Elko_NV	5/18/21 3:00	7.2	5.9	0.5	46.5	9.692	5	3
11	Rowan_NC	5/29/21 20:00	32.7	24.2	2.2	60.5	15.381	5	20
12	Chippewa_WI	6/9/21 0:10	20.2	21.1	1.2	55	17	6	0
13	Pike_PA	6/9/21 22:52	42.3	33.5	2.4	58	18	6	22
14	Jones_NC	6/15/21 19:04	59.2	73.2	3.2	65	19	6	19
15	Meriwether_GA	6/15/22 23:10	51.3	42.3	2.7	60.5	19	6	23
16	Madison_AL	6/15/22 21:00	49.2	42.8	3.1	60.5	17	6	21
17	Lawrence_AL	5/2/22 20:08	41.6	35.6	2.8	60	14	5	20
18	Cayuga_NY	5/16/22 16:40	25.8	15.6	2.1	54.5	10.667	5	16
19	Sampson_NC	6/1/22 23:02	14.8	8.2	1.1	53	13	6	23
20	Washington_NC	6/3/22 18:24	59.4	80.5	3.3	60.5	18.438	6	18
21	Madison_MS	6/16/22 23:18	60.6	38.4	3.2	60.5	19	6	23
22	Allegheny_PA	6/22/22 20:24	49.7	26.5	2.6	56	19	6	20
23	Oconee_GA	3/18/20 23:10	27	21.6	3.2	56	10	3	23
24	Jackson_MS	6/24/22 19:18	21.1	9.3	1.6	54.5	13	6	19
25	Carroll_MD	7/12/22 20:20	49.9	39	3.1	59	16	7	20

Table 3: Data frame of MRMS Radar product values for positive downburst cases. This was developed using python code including a separate case dictionary for the positive downburst cases.

	case_name	**time_stamp**	**VIL**	**VII**	**VIL_Density**	**Reflectivity_-10C**	**EchoTop_30**	**month**	**hour**

0	Knox_TN	2020-03-10 20:38:37	1.3	-1	0.3	23	3.525	3	20
1	Monroe_IN	2021-04-07 18:04:40	3.3	1.5	0.4	40	8	4	18
2	Hoke_NC	2021-05-07 10:24:40	37.4	35.5	3.1	58	13	5	10
3	Bay_FL	2020-06-03 19:56:39	19.6	2.4	2	48.5	8.75	6	19
4	Somerset_PA	2020-07-12 17:50:35	26.1	8.9	2.7	57	10	7	17
5	Orangeburg_SC	2020-08-21 10:26:38	19.1	2.6	2	45.5	11.059	8	10
6	Tuscaloosa_AL	2020-05-28 22:34:37	20.4	8.4	2.1	51.5	10	5	22
7	Grant_IN	2021-06-18 19:42:39	53.6	35.5	2.8	57.5	19	6	19
8	Mifflin_PA	2021-07-03 23:34:41	4.9	0.9	0.6	34.5	8.5	7	23
9	Harrison_TX	2021-08-18 04:18:39	10.1	0.8	0.9	36	9	8	4
10	Spotsylvania_VA	2022-05-15 23:00:40	13.4	1.6	1.2	44.5	7.8	5	23
11	Rapides_LA	2021-09-02 21:36:40	17.3	6	1.4	49.5	11.333	9	21
12	Sarasota_FL	2022-06-11 18:44:38	12.4	2.2	1.2	44.5	11	6	18
13	Laurens_SC	2022-06-28 22:50:41	27.3	9.9	2.6	57.5	12	6	22
14	Moore_NC	2022-07-15 22:18:41	30.2	10.4	2.3	55	14	7	22
15	Brown_OH	2022-08-07 19:32:41	15.2	3.4	1.5	46	11	8	19
16	Bulloch_GA	2022-09-03 18:28:40	12.9	3.7	1.1	44	15	9	18
17	Charles_MD	2020-06-20 18:14:41	26.9	8.9	2.9	59	13	6	18
18	Washington_AK	2020-07-04 19:28:37	9.1	0.6	1.1	37	8	7	19
19	Dyer_TN	2020-08-11 19:28:34	44.1	23.5	2.7	55	17	8	19

Table 4: Data frame of MRMS Radar product values for null cases. This was developed using python code including a separate case dictionary for the null cases.

Figures

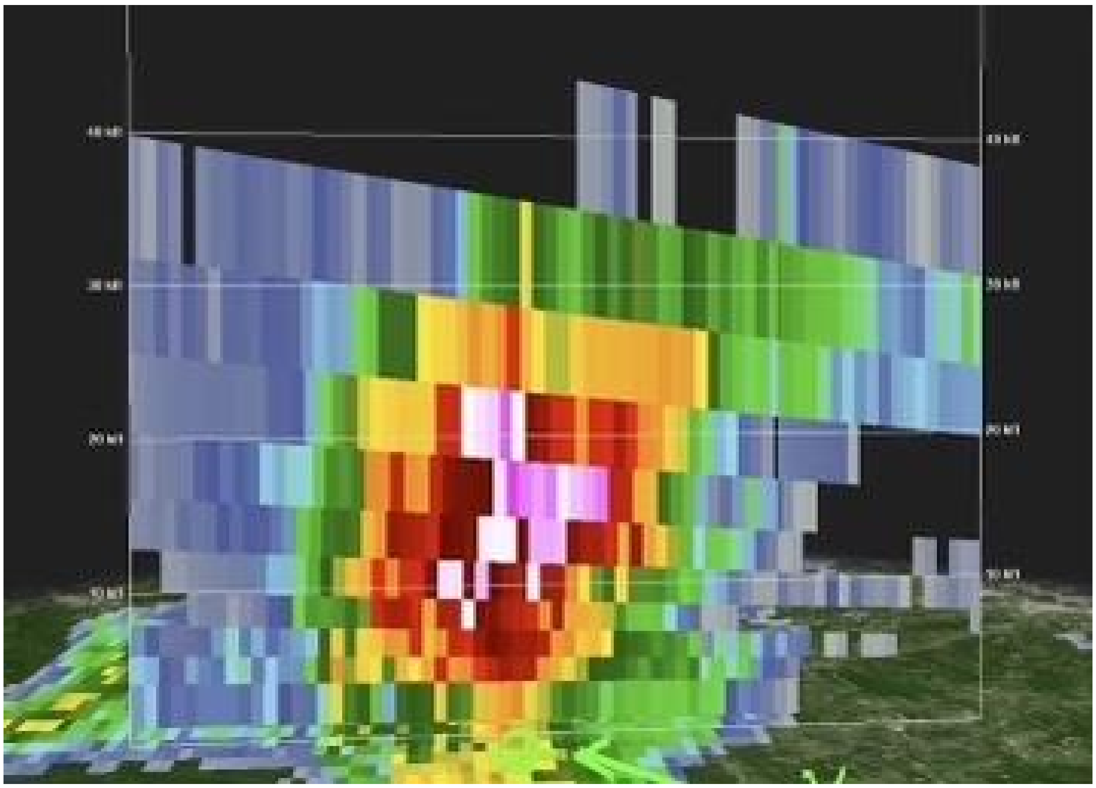

Figure 1: Vertical cross-section in GR2 Analyst depicting the wet downburst the student researcher experienced in Asheville, NC, August 9th, 2012.

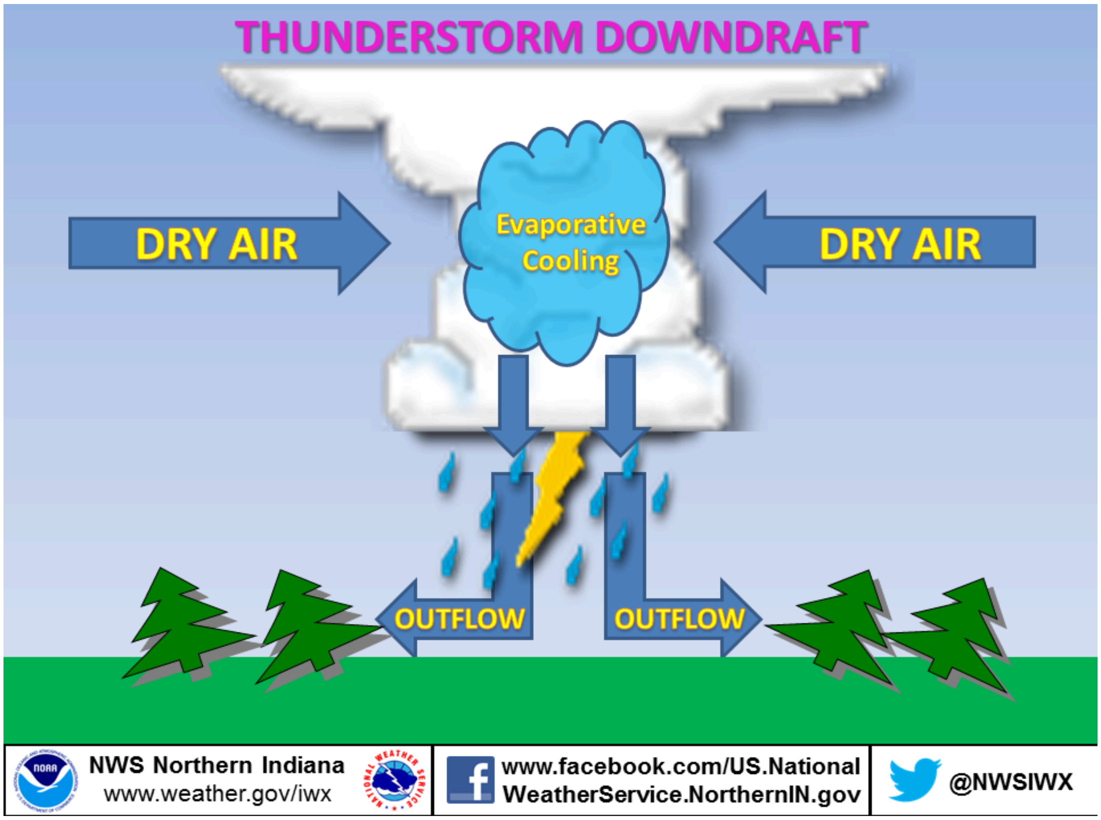

Figure 2: National Weather Service (NWS) infographic depicting the occurrence of a downburst, which is a subclass of severe straight line winds (US Department of Commerce, N., Straight-Line Winds vs. Tornado).

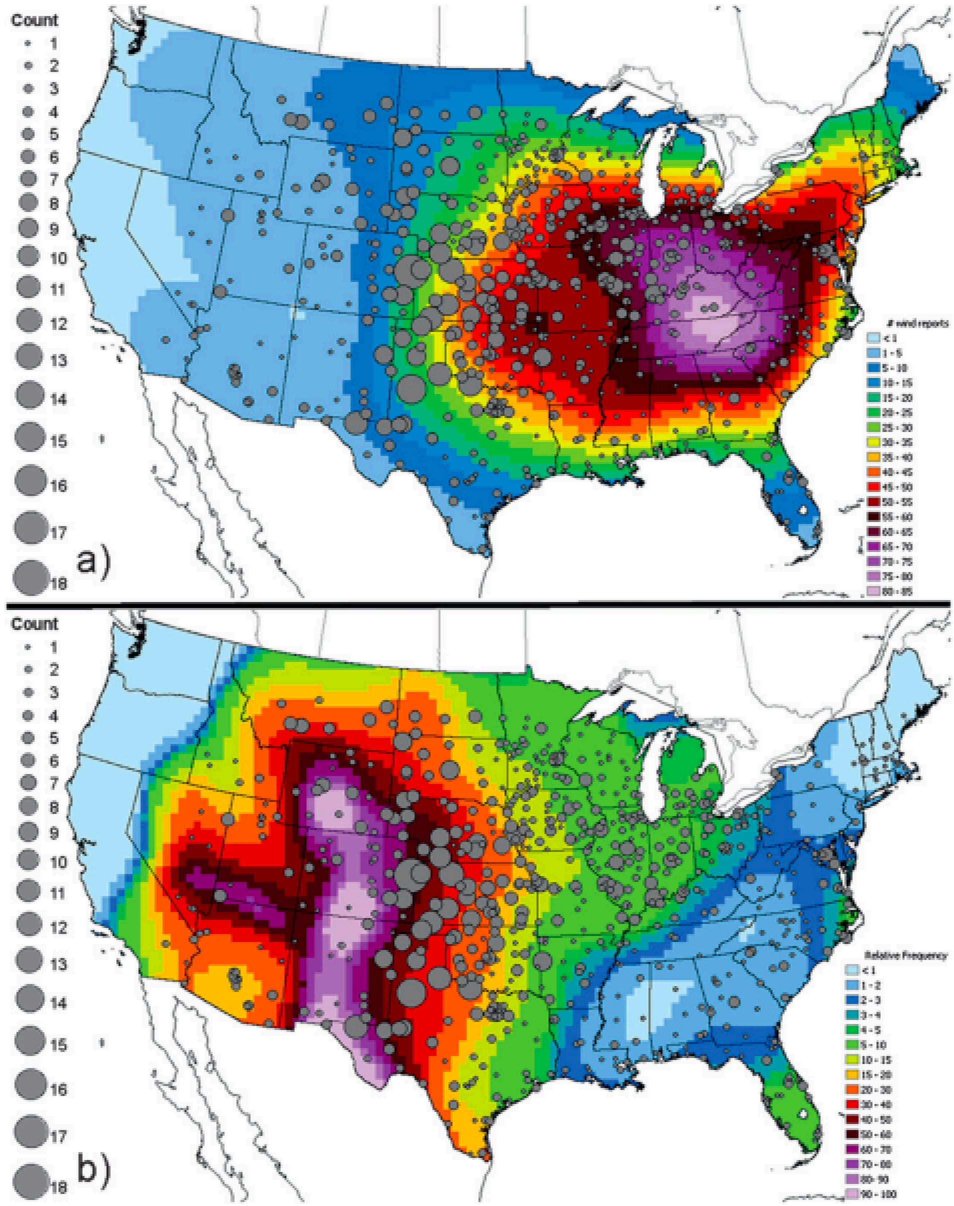

FIG. 6. (a) As in Fig. 1, but the kernel density estimation (40-km grid) of all severe wind reports in the *Storm Data* severe wind database during 2003–09 is shaded. Wind report count normalized to 10 yr. (b) As in (a), but the kernel density estimation of ASOS/AWOS measured ≥25.7 m s^{-1} (50 kt) wind gusts relative to all severe wind reports (92 652) in the *Storm Data* severe thunderstorm wind database during 2003–09 is shaded. The low kernel density estimate values over much of CA, OR, and WA are due to insufficient ASOS/AWOS kernel density data being calculated over those states.

Figure 3:
Adapted from Smith et al. (2013). Figures depict a discrepancy in the location and frequency of severe wind event reports and ASOS/AWOS station reports during the research period of 2003-2009.

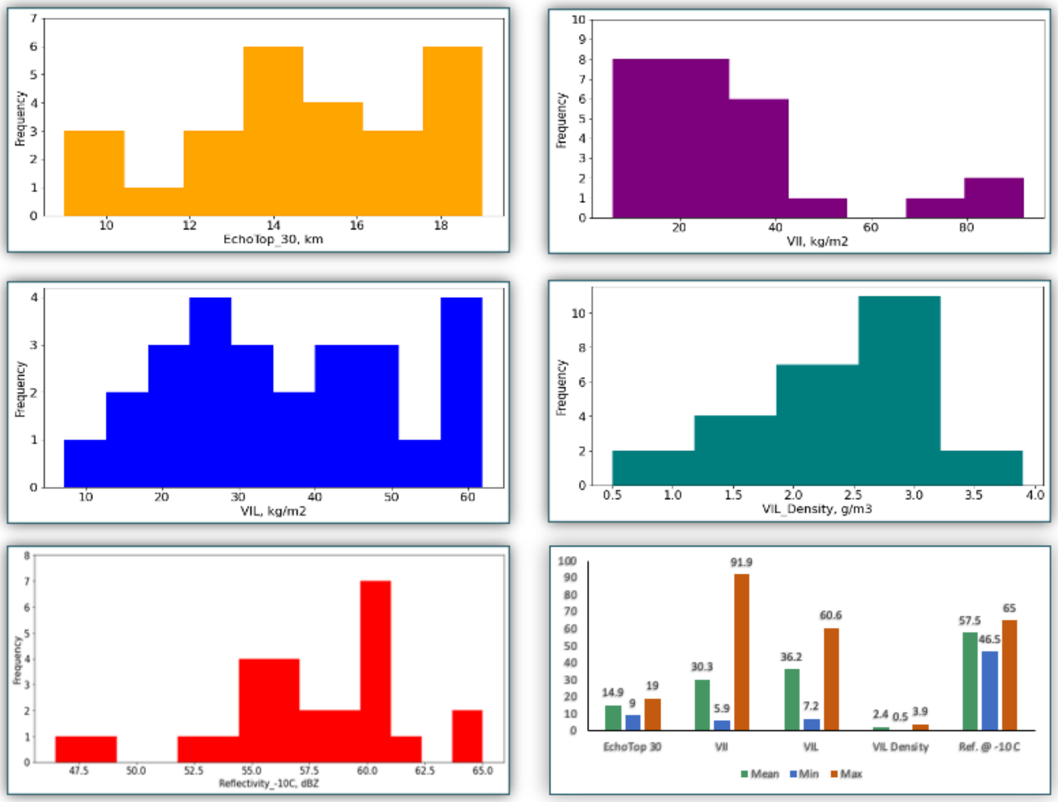

Figure 4: Histogram and statistical analysis charts for the downburst sample set. Left to right, top to bottom: EchoTop 30, VII, VIL, VILD, Reflectivity_-10°C, statistical analysis chart.

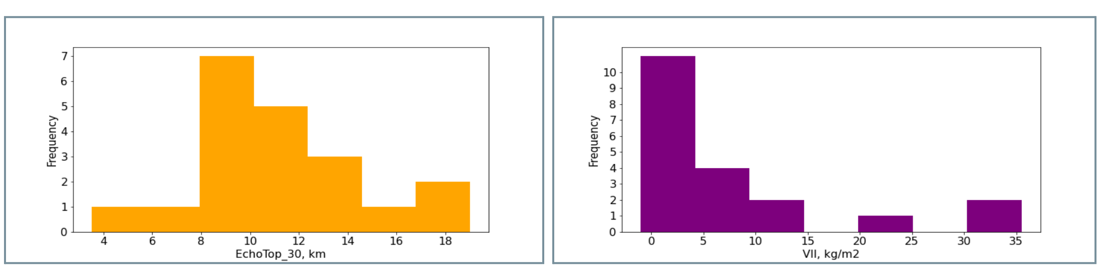

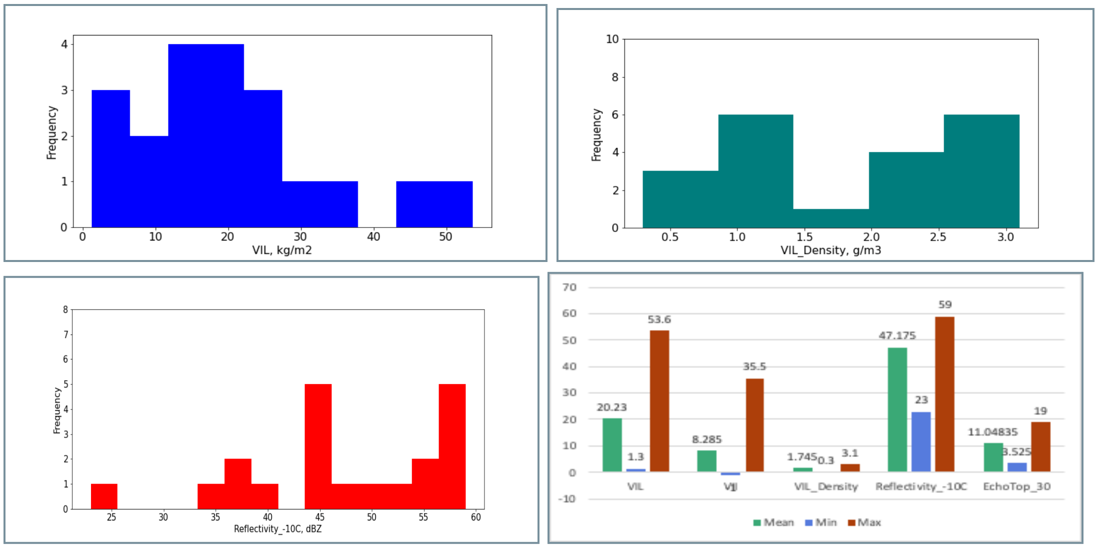

Figure 5: Histogram and statistical analysis charts for the non-severe sample set. Left to right, top to bottom: EchoTop 30, VII, VIL, VILD, Reflectivity_-10°C, statistical analysis chart.

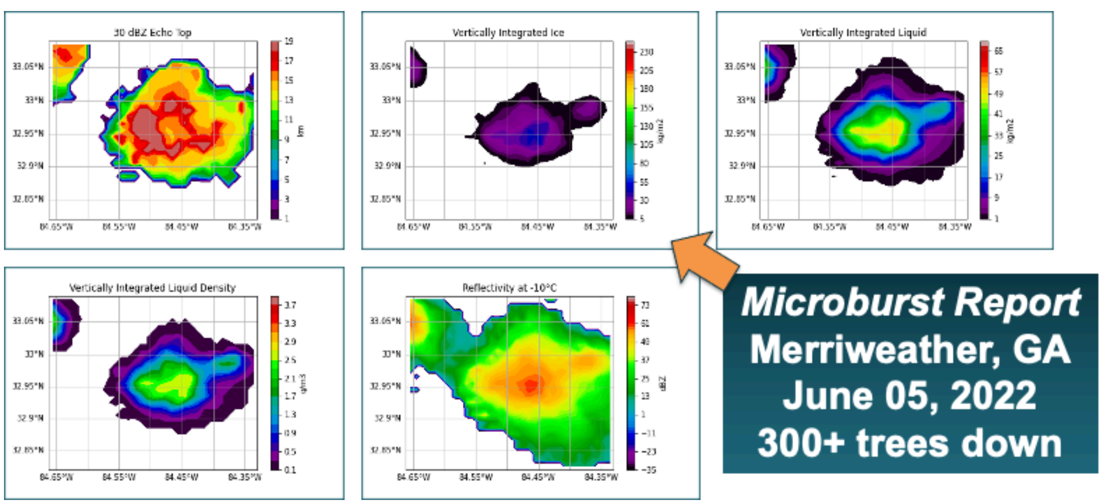

Figure 6: Sample of plots for downburst cases using MRMS Radar Products. These plots depict a microburst that occurred in Merriweather, GA on June 05, 2022. The storm occurred at 2322 Z UTC and downed 300+ trees.
Left to right, top to bottom: EchoTop 30, VII, VIL, VILD, Reflectivity_-10°C.

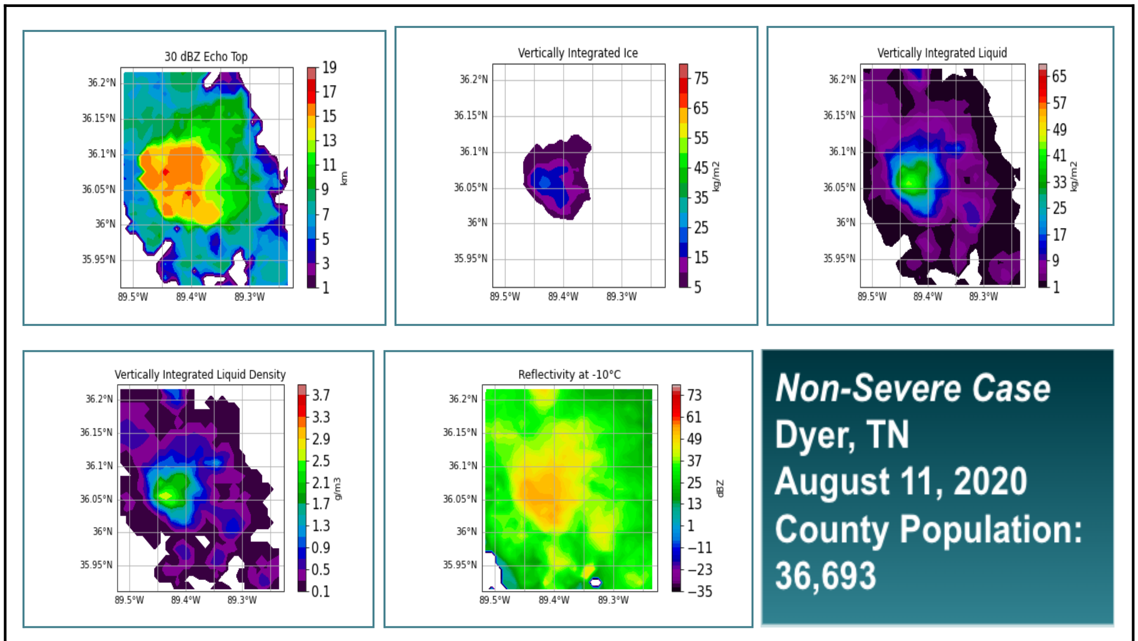

Figure 7: Sample of plots for non-severe cases using MRMS Radar Products. These plots depict a non-severe thunderstorm that occurred in Dyer, TN on August 11, 2020. The storm occurred at 1928 Z UTC.
Left to right, top to bottom: EchoTop 30, VII, VIL, VILD, Reflectivity_-10°C.

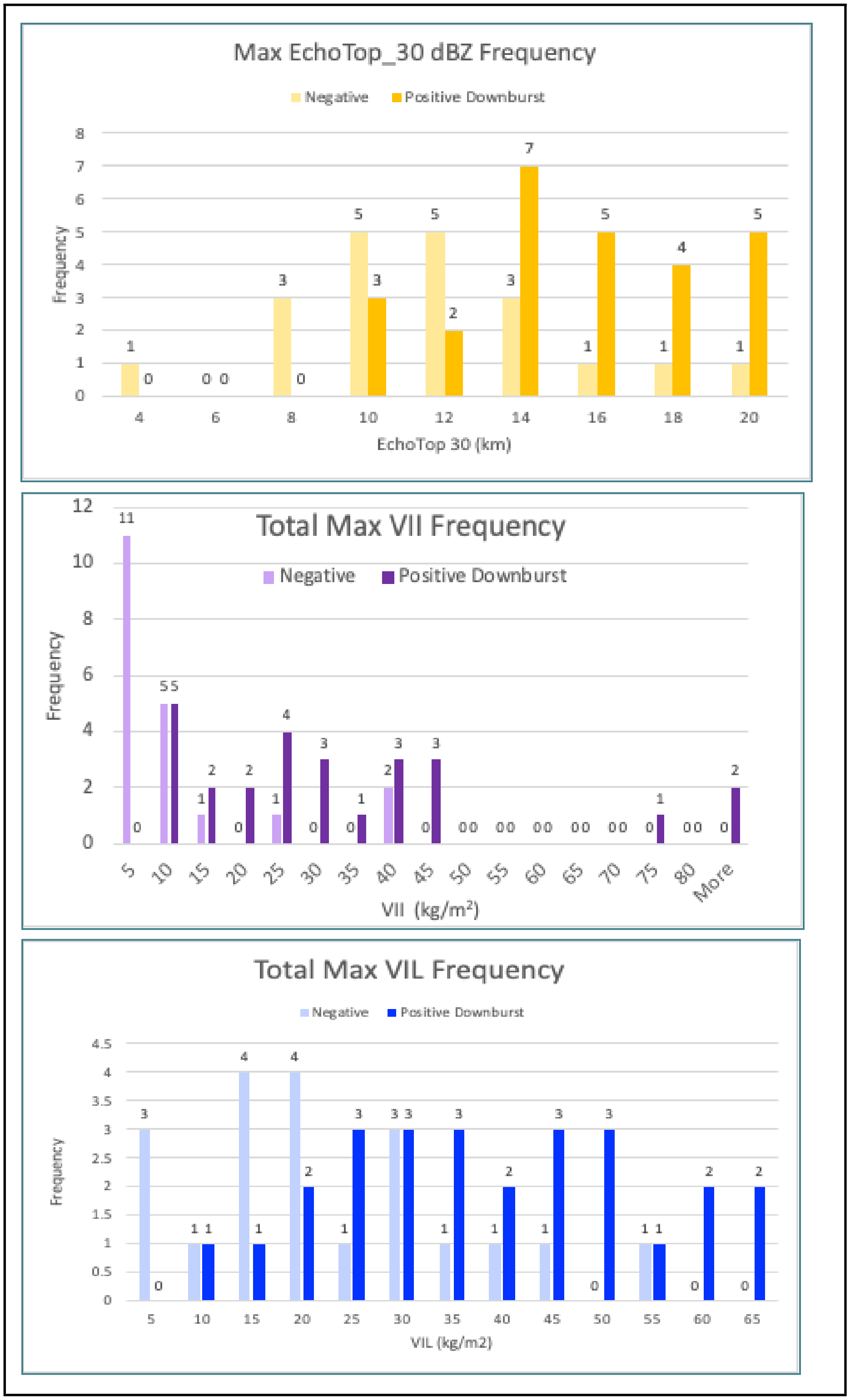
Max EchoTop_30 dBZ Frequency
Negative
Positive Downburst
Frequency
EchoTop 30 (km)
Total Max VII Frequency
Negative
Positive Downburst
Frequency
VII (kg/m²)
Total Max VIL Frequency
Negative
Positive Downburst
Frequency
VIL (kg/m2)

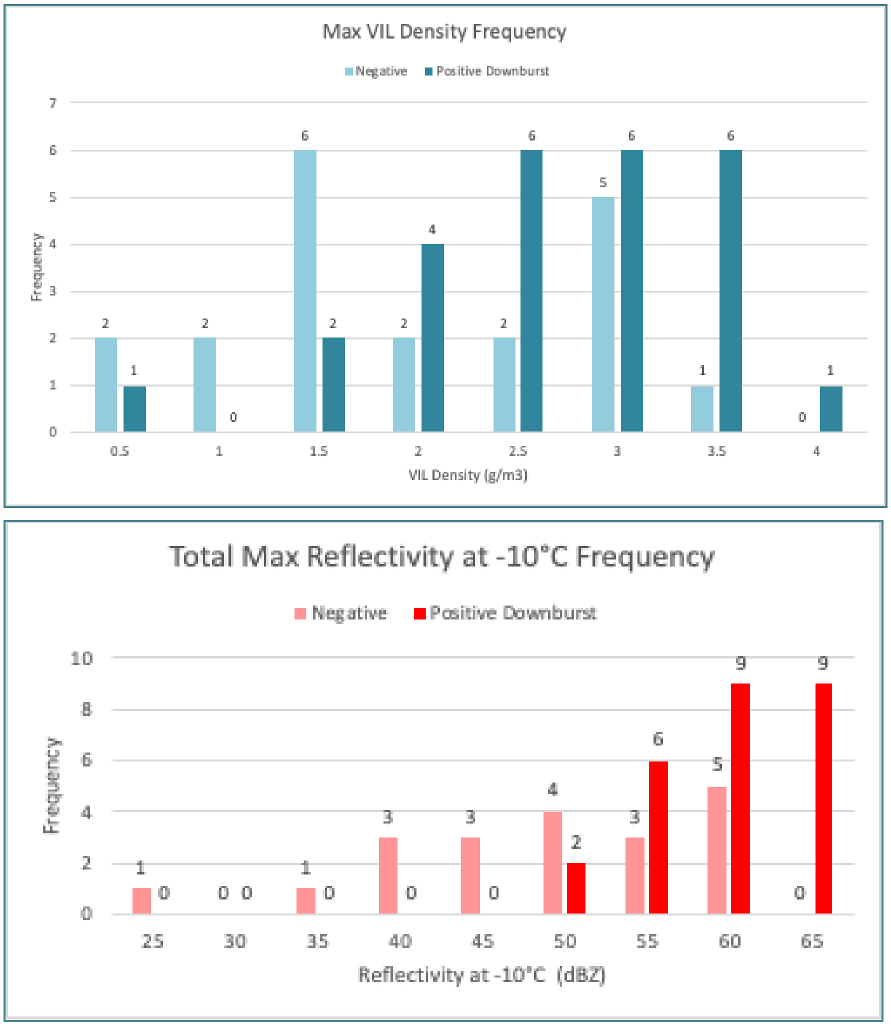

Figure 8: Histogram charts with combined data from both the downburst and null data sets. Top to bottom: EchoTop 30, VII, VIL, VILD, Reflectivity_-10°C.

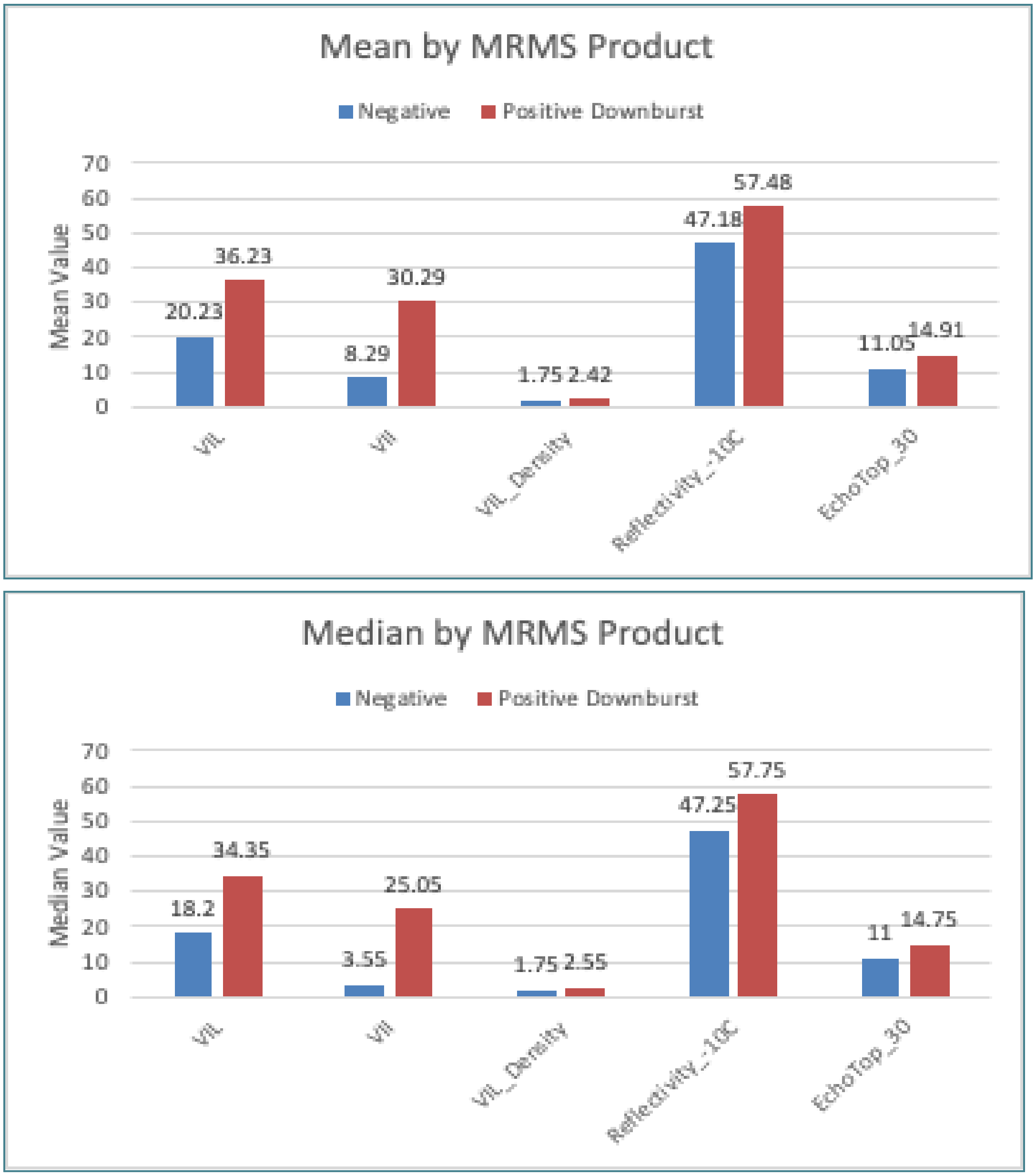

Figure 9: Combined statistical analysis plots of both downburst and non-severe data sets. The top chart represents the mean values for each data set by product, and the bottom chart represents median values for each data set by product.